Received: 20 December 2023 | Revised: 7 February 2024 | Accepted: 15 February 2024

DOI: 10.1002/dneu.22935

RESEARCH ARTICLE

WILEY

S100Z is expressed in a lateral subpopulation of olfactory receptor neurons in the main olfactory system of *Xenopus laevis*

Melina Kahl | **Thomas Offner** | **Alena Trendel** | **Lukas Weiss** | **Ivan Manzini** | **Thomas Hassenklöver**

Institute of Animal Physiology, Department of Animal Physiology and Molecular Biomedicine, Justus-Liebig-University Giessen, Giessen, Germany

Correspondence
Thomas Hassenklöver, Institute of Animal Physiology, Department of Animal Physiology and Molecular Biomedicine, Justus-Liebig-University Giessen, 35392, Giessen, Germany.
Email: thomas.hassenkloever@physzool.bio.uni-giessen.de

Present addresses
Thomas Offner, Zebrafish Neurobiology, European Neuroscience Institute, Göttingen, Germany.
Lukas Weiss, Department of Ecology and Evolutionary Biology, Princeton University, Princeton, NJ, USA.

Funding information
Deutsche Forschungsgemeinschaft, Grant/Award Number: 4113/4-1

Abstract

In contrast to other S100 protein members, the function of S100 calcium-binding protein Z (S100Z) remains largely uncharacterized. It is expressed in the olfactory epithelium of fish, and it is closely associated with the vomeronasal organ (VNO) in mammals. In this study, we analyzed the expression pattern of S100Z in the olfactory system of the anuran amphibian *Xenopus laevis*. Using immunohistochemistry in whole mount and slice preparations of the larval olfactory system, we found exclusive S100Z expression in a subpopulation of olfactory receptor neurons (ORNs) of the main olfactory epithelium (MOE). S100Z expression was not co-localized with TP63 and cytokeratin type II, ruling out basal cell and supporting cell identity. The distribution of S100Z-expressing ORNs was laterally biased, and their average number was significantly increased in the lateral half of the olfactory epithelium. The axons of S100Z-positive neurons projected exclusively into the lateral and intermediate glomerular clusters of the main olfactory bulb (OB). Even after metamorphic restructuring of the olfactory system, S100Z expression was restricted to a neuronal subpopulation of the MOE, which was then located in the newly formed middle cavity. An axonal projection into the ventro-lateral OB persisted also in postmetamorphic frogs. In summary, S100Z is exclusively associated with the main olfactory system in the amphibian *Xenopus* and not with the VNO as in mammals, despite the presence of a separate accessory olfactory system in both classes.

KEYWORDS
amphibian, calcium-binding protein, frog, larval, olfaction, tadpole, vomeronasal organ

1 | INTRODUCTION

Calcium (Ca^{2+}) is a ubiquitous intracellular messenger, which influences and regulates a variety of cellular processes in multifaceted ways (Berridge et al., 2003; Carafoli et al., 2001). Ca^{2+} signaling fundamentally depends on intracellular Ca^{2+} concentration changes in complex spatio-temporal patterns (Berridge et al., 2000). These signals are detected, modulated, and transduced by a diverse set of molecular elements, including Ca^{2+}-binding proteins, to regulate cell physiology (Elíes et al., 2019; Yáñez et al., 2012). The superfamily of Ca^{2+}-binding proteins with EF-hand motif plays a key role in

this process by buffering cytosolic Ca^{2+}, fine-tuning the spatial and temporal properties of Ca^{2+} signals and mediating functional changes (Schwaller, 2020).

The S100 protein family is a distinct class of EF-hand Ca^{2+}-binding proteins and has only been identified in vertebrates (Gonzalez et al., 2020). It consists of more than 20 known members that exhibit cell type-specific expression (Gonzalez et al., 2020). A shared feature of S100 proteins is a characteristic dimeric architecture, where each monomer contains two EF-hand motifs connected by a flexible linker region (Santamaria-Kisiel et al., 2006). Binding of Ca^{2+} leads to conformational changes in these regions that ultimately facilitate the interaction with target proteins to regulate their activity (Santamaria-Kisiel et al., 2006). S100 proteins are involved in cell differentiation and proliferation, cell motility, apoptosis, regulation of enzymes, immune homeostasis, and modulation of membrane-cytoskeletal interactions, among others (Gonzalez et al., 2020). It has been well-established in both humans and rodents that S100 dysregulation can be the cause of various diseases such as cancer, inflammatory/autoimmune conditions, diabetes, and neurodegenerative diseases (Gonzalez et al., 2020; Singh & Ali, 2022). S100 proteins play an important role also in neurons, where they directly modulate ion channels shaping neuronal activity (Hermann et al., 2012). Notably, S100 proteins not only act as intracellular regulators but some members are secreted into extracellular space to exert effects on distant cells (Donato, 2003).

S100 calcium-binding protein Z (*s100z*) is a less well-characterized member of the S100 protein family. The function of S100Z is still largely unknown, but the studies available suggest an important role in the olfactory system. In larval zebrafish, *s100z* expression is exclusively found in the olfactory placode and is restricted to a subpopulation of cells, presumably neurons (Kraemer et al., 2008). In the olfactory organ of adult zebrafish, the regions comprising olfactory receptor neurons (ORNs) express *s100z* (Dieris et al., 2021). In mammals, *s100z* is associated with the accessory olfactory system, specifically the vomeronasal organ (VNO; Hecker et al., 2019). Notably, the evolutionary reduction/loss of the VNO in aquatic mammals, several bats, and primates coincides with an inactivation of the *s100z* gene (Hecker et al., 2019).

During tetrapod evolution, the olfactory system shows a trend toward functional and morphological segregation into distinct subsystems (Bear et al., 2016). While teleost fish have a peripheral olfactory organ with a single sensory surface, tetrapods have distinct main and accessory olfactory organs: the main olfactory epithelium (MOE) and the VNO (Bear et al., 2016; Mohrhardt et al., 2018; Weiss et al., 2021). The different subsystems are also separated at the level of the brain, where the olfactory projections target a main and an accessory olfactory bulb (AOB; Bear et al., 2016; Mohrhardt et al., 2018; Weiss et al., 2021). Olfactory sensory neurons associated with these subsystems differ in their morphology and molecular properties, like olfactory receptor gene family expression and transduction machinery (Bear et al., 2016; Mohrhardt et al., 2018; Weiss et al., 2021). Although amphibians present a distinct VNO, as other tetrapods, the organizational division is incomplete and ORNs with different molecular identities are intermingled in the MOE (Date-Ito et al., 2008; Gliem et al., 2013; Sansone, Hassenklöver, et al., 2014; Sansone, Syed, et al., 2014; Syed et al., 2013; Weiss et al., 2021).

Since *s100z* has been linked to the VNO in mammals, this raises the question of how it is distributed in basal tetrapods, the amphibians. Here, we examined whether the expression of *s100z* is always strictly associated with the VNO in an anuran amphibian. We applied immunohistochemistry to investigate the expression pattern of S100Z in the pre- and postmetamorphic olfactory system of *Xenopus laevis*.

2 | MATERIALS AND METHODS

2.1 | Animals

Wildtype albino *X. laevis* (both sexes) and transgenic albino paired box 6 (*pax6*)-green fluorescent protein (GFP) [Xla.Tg (*pax6*: GFP; *cmv*: DsRED)^{Papal} (xenopusresource.org) bred into an albino background in our lab] *X. laevis* were used. They were kept and bred at the animal husbandry facility of the Institute of Animal Physiology of the Justus-Liebig-University Giessen. Tanks with volumes of 1.8−7.5 L and constant water circulation at 19−22°C were used. Tadpoles were fed with a mixture of *Spirulina* and *Chlorella* algae (MS-Tierbedarf) and frogs with ESF 10 Krallenfrosch Extrudat (Granovit AG). Tadpoles of stages 48−52 were used as a representative of the premetamorphic developmental phase, and froglets of stage 66 were used as a representative of the post-metamorphic developmental phase (Nieuwkoop & Faber, 1994). All animal procedures were performed in accordance with the guidelines of Laboratory animal research of the Institutional Care and Use Committee of the University of Giessen (649_M).

Before experimental procedures, animals were anesthetized using 0.02% MS-222 (ethyl 3-aminobenzoate methanesulfonate, TCI Tokio Chemicals) in tap water. Anesthetized animals were killed by severing the transition between the brainstem and spinal cord. Tissue blocks containing the noses and the rostral part of the telencephalon were excised.

2.2 | General labeling of ORNs

In some samples, we labeled sensory neurons by using a biocytin backfill. Within the tissue blocks, we transected both

ONs with fine scissors without damaging surrounding tissue and placed Biocytin (ε-biotinoyl-L-lysine, Molecular Probes, ThermoFisher Scientific) crystals into the lesioned ONs. With this approach, all ORNs of the olfactory organ that have an axon at the transection site were labeled. The lesion was closed with tissue adhesive (Histoacryl L; Braun) and tissue blocks were incubated for 1 h at room temperature in frog Ringer solution (98 mM NaCl, 2 mM KCl, 1 mM $CaCl_2$, 2 mM $MgCl_2$, 5 mM Na-pyruvate, 5 mM glucose, 10 mM HEPES, pH 7.8, osmolarity of 230 mOsmol/l).

2.3 | Fixation

All samples were fixed in 4% formaldehyde for 1 h at room temperature and washed three times, each 10 min, with phosphate-buffered saline (PBS: 137 mM NaCl, 2.7 mM KCl, 8 mM Na_2HPO_4, 1.4 mM KH_2PO_4, dissolved in purified water, pH 7.4).

2.4 | Whole mount and tissue slice preparation

We either used whole mount preparations or tissue slices for labeling. In whole mounts, we investigated the whole olfactory system by cutting the olfactory nerves (ONs) close to the noses and extracting the entire brain from the tissue block. The complete olfactory epithelium was preserved and processed independently. We did not use any embedding medium for the tissue blocks. For the preparation of tissue slices of the olfactory system, we glued tissue blocks directly onto the stage of a half-automatic vibratome (VT1200S; Leica Biosystems). Tissue blocks containing the olfactory epithelium were sliced horizontally at 200−250 μm thickness, whereas OB slices were sliced at 330 μm thickness.

2.5 | Immunohistochemistry

All tissues were permeabilized using phosphate-buffered saline containing 0.2% Triton-X100 (PBST; Carl Roth) three times, each 10 min, and non-specific binding was blocked with 2% normal goat serum (NGS; MP Biomedicals) for 1 h at room temperature. The samples were incubated with primary antibodies (1:100) in PBST and 2% NGS at 4˚C for 68 to 72 h with one or two of the following antibodies: anti-*Homo sapiens* S100Z (MBS2033797, polyclonal, derived from rabbit; BioTrend); anti-*X. laevis* cytokeratin type II (Cytok II; 1h5, RRID:AB_528323, monoclonal, derived from mouse; deposited to the Developmental Studies Hybridoma Bank by Klymkowsky, M.); anti-calretinin (6B3, RRID:AB_10000320 monoclonal, derived from mouse, Swant); anti-neural cell adhesion molecule 1 (NCAM1; 4d, RRID:AB_528389, monoclonal, derived from mouse, deposited to the Developmental Studies Hybridoma Bank by Rutishauser, U.); anti-beta tubulin (TUBB; E7, RRID:AB_528499, monoclonal, derived from mouse, deposited to the Developmental Studies Hybridoma Bank by Klymkowsky, M.); anti-TP63 (ab735, RRID:AB_305870, monoclonal, derived from mouse, Abcam). The human S100Z protein (NCBI Reference Sequence: XP_054207898.1) shows an amino acid identity similarity of ∼75% and ∼87% positives, compared to the translated mRNA sequence of the *X. laevis* L/S homeologs (NM_001097818.2, XM_041580516.1; tblastn). Green fluorescent protein signals were enhanced with anti-GFP (ab1218, RRID:AB_298911, monoclonal, derived from mouse; Abcam). The primary antibodies were washed off with PBS three times, each 10 min.

The samples with biocytin-backfilled ORNs were additionally incubated in Alexa 488-conjugated streptavidin (Molecular Probes, Thermo Fisher Scientific) at a final concentration of 5 μg/mL in PBST for 5 h and repeatedly rinsed in PBS. They were incubated with the secondary antibodies Alexa Fluor 594 goat anti-rabbit (Invitrogen, Thermo Fisher Scientific; 1:250) in PBS with 2% NGS at 4˚C for 68 to 72 h.

All other samples were incubated with the secondary antibodies Alexa Fluor 488 goat-anti mouse or/and Alexa Fluor 488 or 594 goat-anti rabbit (Invitrogen, Thermo Fisher Scientific; 1:250) in PBS with 2% NGS at 4˚C for 68 to 72 h. The secondary antibodies were washed off with PBS three times, each 10 min.

In samples with only one primary antibody application, cell nuclei were labeled with 10 μg/mL propidium iodide (Molecular Probes, Thermo Fisher Scientific) for 15 min and subsequently washed three times with PBS, each 10 min. It was standard procedure to perform negative antibody controls.

2.6 | Image acquisition and processing

Samples were transferred into a recording chamber in PBS and stabilized with a platinum frame stringed with nylon threads. The OBs were imaged with the ventral surface up and the olfactory epithelia were imaged with the dorsal surface up.

The image stacks were acquired using multiphoton microscopy (A1R MP; Nikon) at an excitation wavelength of 780 nm. Axial resolution of OB and MOE samples was 3 and 2 μm, respectively. Fluorescence emission was detected with three different detectors (blue 400−492 nm, green 500−550 nm, red 601−657 nm). The brightness and contrast of the image stacks were adjusted using the image processing software ImageJ (Schindelin et al., 2012) and median filtering was applied to reduce image noise when

necessary. Pigmentation-derived autofluorescence was mathematically removed by subtracting the blue channel from the other channels using the image calculator function in ImageJ. Images showing the whole olfactory system of adult animals were combined from multiple image stacks using a stitching algorithm (Preibisch et al., 2009).

2.7 | Data analysis

S100Z-positive cells of the MOE were manually counted using ImageJ. The MOE was divided into smaller z-stacks (six to ten substacks) from dorsal to ventral. In all image planes, the basal and apical boundaries of the OE were traced with the freehand tool. These reference outlines were used for the distribution analysis of S100Z-positive cells. Each cell soma showing fluorescence signal was manually outlined using the region of interest (ROI) manager of ImageJ. The absolute position of each cell was defined as the centroid of cell soma outline. The relative position within the MOE was defined as the angle from the center of the fluid-filled nasal cavity. A vector through the average coordinates of the basal and apical boundary regions was identified as a good proxy for the middle of the MOE. We connected the position of each identified cell to the apical boundary central point and calculated the angle to the central vector (see also Figure 3a). An angle of 0° was defined at a position directly in the middle of the lateral to medial axis of the MOE. Negative and positive angles indicated lateral and medial positions, respectively. The distribution pattern of the labeled cells was evaluated in Python (code and data are available at https://doi.org/10.22029/jlupub-18280). We identified and quantified the distribution of biocytin-backfilled ORNs as a control using the same protocol.

2.8 | Statistics

Statistical difference was analyzed using Kruskal–Wallis paired samples test with Bonferroni correction.

3 | RESULTS

3.1 | S100Z expression in the olfactory system of larval *X. laevis*

Immunohistochemical processing of the olfactory system of premetamorphic *X. laevis* with an antibody against S100Z leads to strong labeling in both the MOE and OB (Figure 1). We found S100Z expression in bipolar cells with an apical dendritic knob, throughout the whole MOE, resembling ORNs (Figure 1a). We identified fibers connected to labeled cells as axons that were clearly projecting into the ON and subsequently into glomerular clusters of the OB (Figure 1b). Within the OB, we found no S100Z-positive cell bodies.

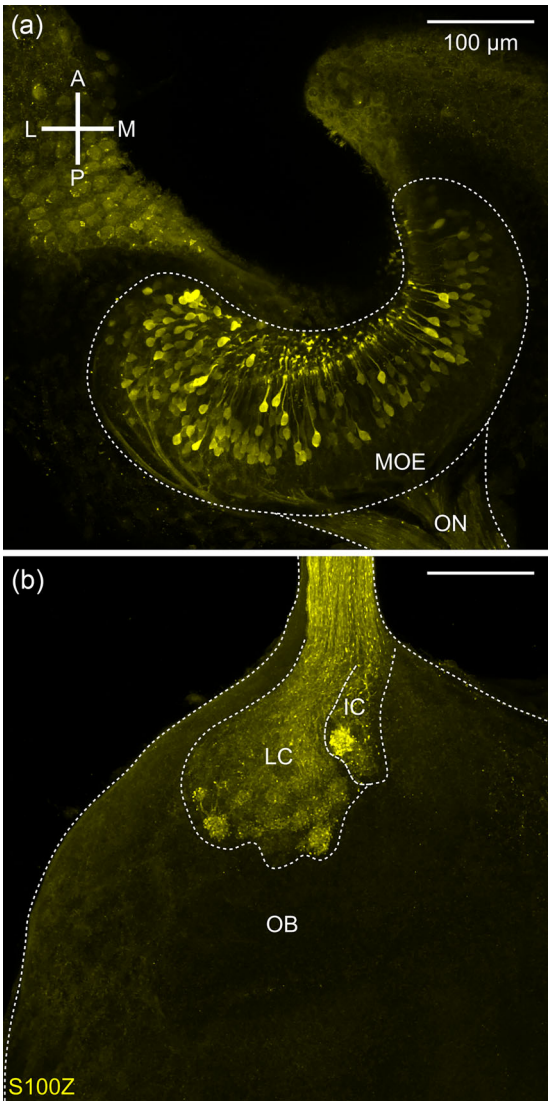

FIGURE 1 S100Z expression in the main olfactory system of larval *Xenopus laevis*. (a) Immunohistochemical staining for S100Z revealed cells with neuron-like morphology, bipolar shape with dendritic knobs, throughout the whole MOE of the peripheral olfactory organ. The axon-like processes of S100Z-positive cells extended into the ON. (b) Axons of S100Z-positive cells projected into glomeruli within the glomerular layer of the OB in premetamorphic tadpoles. No S100Z-positive cell bodies were visible in the different layers of the OB. Structures of the olfactory system and glomerular clusters are outlined with a dotted white line. A, anterior; IC, intermediate cluster; L, lateral; LC, lateral cluster; M, medial; MOE, main olfactory epithelium; OB, olfactory bulb; ON, olfactory nerve; P, posterior.

3.2 | S100Z expression restricted to ORNs

We performed complementary immunohistochemistry in premetamorphic *X. laevis* to confirm the neuronal identity of labeled cells and to check for other cell types that

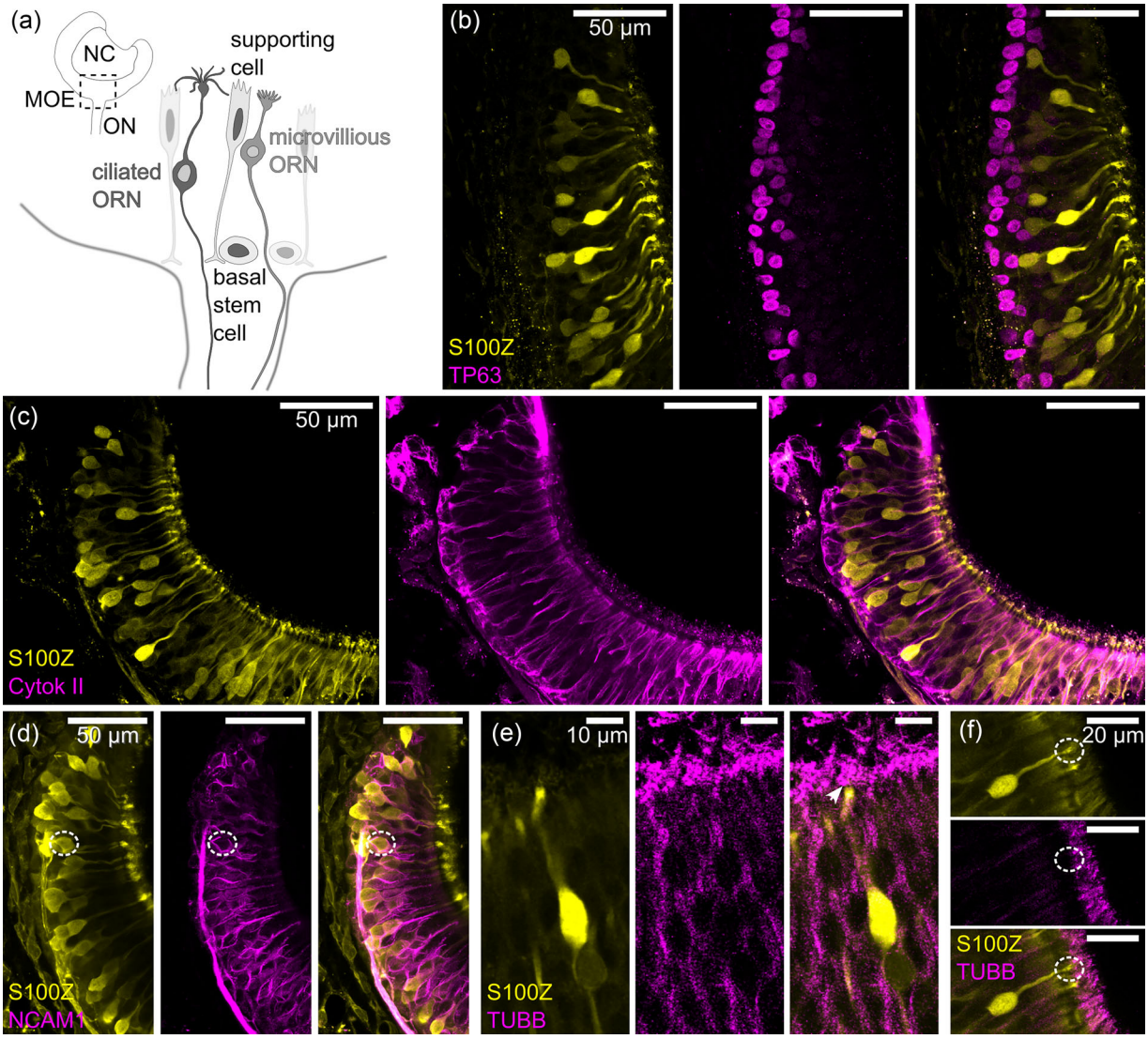

FIGURE 2 S100Z expression exclusively in ORNs. (a) Schematic overview of the peripheral olfactory organ of premetamorphic *X. laevis*. The major cell types of the main olfactory epithelium are highlighted. (b) Stem cell marker TP63 (magenta) was localized in cell nuclei in basal cell layers, highlighting basal stem cells. S100Z-positive cells (yellow) occurred in more intermediate layers of the olfactory epithelium. No co-localization of S100Z and TP63 was found. (c) Supporting cells expressing cytokeratin type II (Cytok II, magenta) did not express S100Z (yellow). (d) Membrane-localized NCAM1 (magenta) is a marker for developing neurons. A subset of S100Z-expressing cells (yellow) was clearly surrounded by NCAM1 immunoreactivity (white dotted circle) and dendrites showed co-localization. (e) Microtubules were labeled with antibodies against beta tubulin (TUBB, magenta). TUBB was found at cellular boundaries and apical appendages, presumably cilia (arrow). S100Z signal only clearly occurred in soma, dendrite, and knob. (f) Individual S100Z-positive neurons show no co-localization of S100Z and TUBB in their dendritic appendages. TUBB expression is expected in cilia, whereby S100Z was located in shorter protrusions from the dendritic knob, potentially indicating microvilli (white dotted circle). MOE, main olfactory epithelium; NC, nasal cavityl; OB, olfactory bulb; ON, olfactory nerve; ORN, olfactory receptor neuron.

potentially express S100Z (Figure 2). Tumor protein 63 (TP63) is expressed in reserve horizontal stem cells in the olfactory epithelium (Schnittke et al., 2015). Antibody labeling against TP63 was localized in cell nuclei in the basal cell layers of the olfactory epithelium, while S100Z-positive cells were located in more intermediate layers (Figure 2b). We found no co-localization of TP63 in S100Z-positive cells.

Supporting cells were labeled with an antibody against Cytok II and revealed their typical morphology with apical cell soma positions and thin processes connecting to the basal lamina of the MOE (Figure 2c). We found no co-localization of labeled supporting cells and S100Z.

An antibody against NCAM1 was used to label immature ORNs within the MOE (Cervino et al., 2017). We found NCAM1 expression in many S100Z-positive cells, and it was

localized to the plasma membrane at the cell soma and in dendritic and axonal processes (Figure 2d).

We applied an antibody against TUBB to check if S100Z-positive neurons possess cilia as dendritic knob appendages. TUBB immunoreactivity was located in the intermediate level of the olfactory epithelium at cell boundaries and in long cilia at the apical interface to the nasal cavity (Figure 2e). In general, the TUBB signal extended more apically than the S100Z signal (arrow). S100Z-immunoreactivity was located in dendrites and the connected knobs of ORNs but was not apparent in TUBB-positive cilia (Figure 2f, white dotted oval). This indicated that S100Z was expressed in microvillars rather than ciliated ORNs.

In summary, we found that S100Z expression occurred exclusively in ORNs within the MOE of premetamorphic *X. laevis* larvae with specific projections into the lateral and intermediate glomerular cluster of the OB.

3.3 | Laterally biased distribution of S100Z-expressing ORNs in the MOE

The fact that projections of S100Z-positive axons were not connecting to the medial OB raises the question how S100Z-expressing ORNs are distributed within the olfactory organ. We manually counted and identified the position of all S100Z-positive ORNs in image stacks of the MOE of premetamorphic animals (n = 11 larvae; Figure 3). For each ORN, we determined the angle from the center of the MOE as a measure of lateral to medial position within the MOE (Figure 3a). The population of S100Z-expressing ORNs showed a bimodal distribution with a strong bias to the lateral side of the MOE (Figure 3b). On average, significantly more S100Z-positive ORNs were found in the lateral half of the olfactory epithelium of each animal than in the medial half (p = .0035, Figure 3c). This was consistently found in every animal analyzed (Figure 3d). We counted and identified biocytin-positive cells (n = 4 larvae) to test if ORNs were generally more frequently found in the lateral MOE. The distribution of the total ORN population is approximately symmetric and centered around the middle of the MOE (Figure 3b). No significant difference between the mean number of biocytin-positive cells was apparent between the lateral and medial MOE (p = .08326). The comparison of biocytin- and S100Z-positive distributions also suggested that the centrally located ORNs had a reduced probability for S100Z expression. On an apical to basal axis, the lateral and medial S100Z-positive ORNs did not differ in distribution (Figure 3e). Nevertheless, we found a tendency that S100Z-expressing ORN somata were located more apically in more ventral layers on the medial half of the MOE (Figure 3f).

3.4 | S100Z expression in ORNs without axon and *pax6*-expressing cells

We wanted to obtain more information about the maturity of S100Z-expressing neurons and labeled ORNs through their axons via transection of the ON using a biocytin backfill in premetamorphic *X. laevis* (Figure 4a–c). All ORNs with a well-developed axon at the transection site were labeled. Growing neurons that have not developed an extended axon yet are excluded from this labeling approach. We found that a biocytin backfill led to the widespread labeling of ORNs in the MOE (Figure 4a). Concurrent labeling with S100Z in a subset of biocytin-filled neurons supports our previous finding of ORN-specific expression of S100Z (Figure 4a). We found partially overlapping subsets of ORNs labeled with biocytin and S100Z (Figure 4a). Furthermore, the biocytin-streptavidin backfill was observable in the axonal projections of ORNs into the AOB and in all glomerular clusters of the OB, namely, the lateral (LC), intermediate (IC), small (SC), and medial clusters (MC; Figure 4b). Only in the LC and IC, we found co-localization of S100Z and biocytin-streptavidin but not in all glomeruli (Figure 4b). Notably, no S100Z signal occurred in the projections to glomeruli of the AOB (Figure 4b). Consistent with this, we also found generally no S100Z expression in the peripheral VNO (Figure 4c). S100Z expression was always restricted to the MOE.

pax6 is one of the main developmental regulators in vertebrates and cellular expression has been well-studied in the OB, pallium, and telencephalon of *Xenopus* (Daume et al., 2022; Moreno et al., 2008; Stoykova & Gruss, 1994). We used an albino *pax6*-GFP transgenic *Xenopus* line to visualize developing neurons within the premetamorphic MOE. *pax6*-dependent GFP expression was distributed throughout the whole MOE (Figure 4d). Many S100Z-expressing cells showed co-localization with *pax6*-GFP signal, but we also found S100Z-positive cells without *pax6* expression (Figure 4d). The axonal projections of *pax6*-positive ORNs projected broadly into all glomerular clusters of the OB (Figure 4e). A subset of *pax6*-positive glomeruli in the LC showed co-localization with S100Z, while another group was devoid of S100Z (Figure 4e). Note that also *pax6*-positive cell somata were found in the mitral and granule cell layers of OB, and that these exhibited no S100Z signal.

Our findings demonstrate that S100Z was expressed in a subgroup of *pax6*-positive ORNs as well as in developing

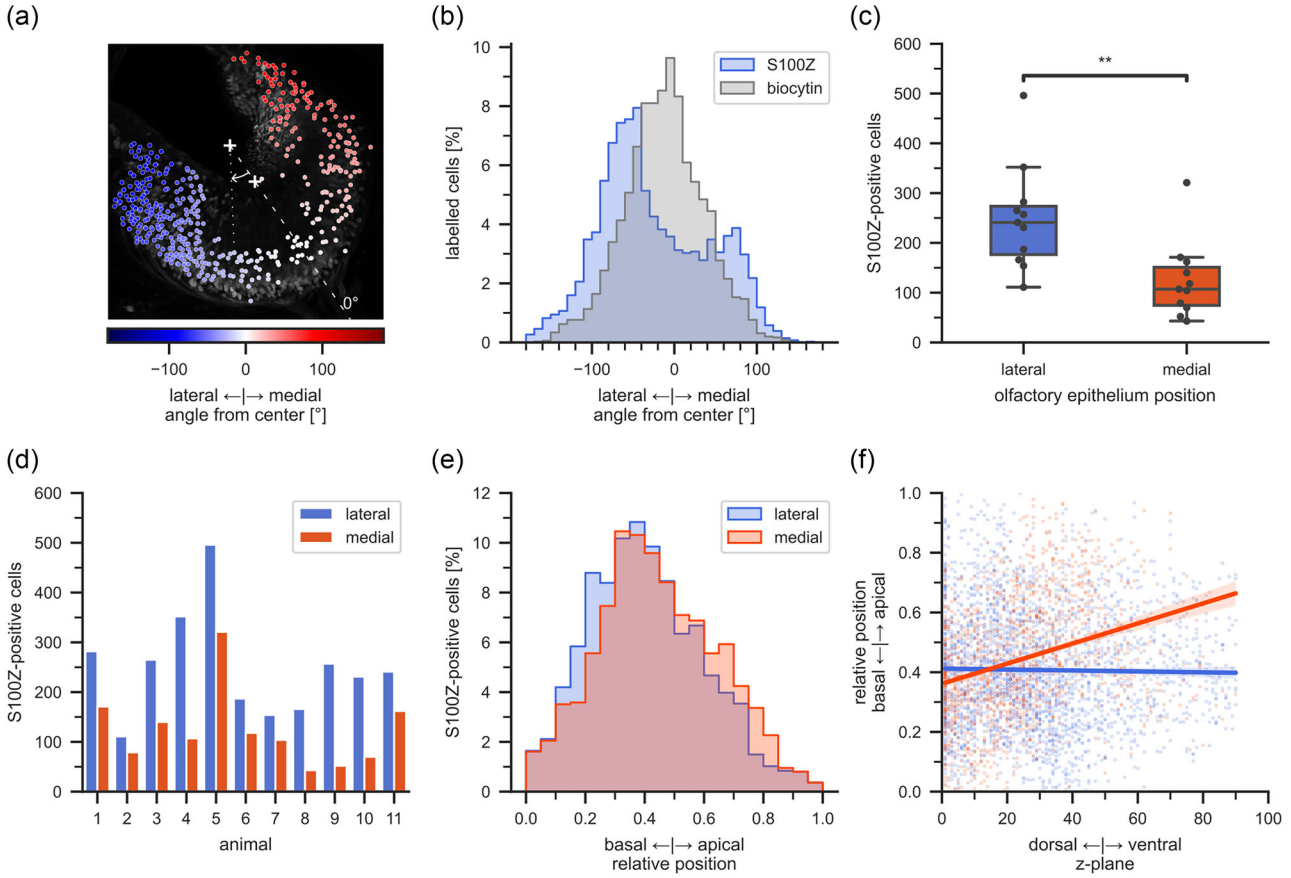

FIGURE 3 Laterally shifted distribution of S100Z-positive cells. (a) Maximum projection of a larval *X. laevis* MOE with an overlay of all S100Z-positive cells. The color gradient from blue (lateral) to red (medial) indicates the angular position within the MOE (zero equals the middle of the MOE). Crosses mark the average coordinates of the manually drawn apical and basal MOE boundaries. Angles were determined between each cell position and the vector that defined the middle of the MOE (dashed line). (b) The bimodal distribution of S100Z-positive cells (blue) was shifted toward a lateral position ($n = 11$ larvae). The general ORN population was labeled via a biocytin backfill and showed a unimodal distribution centered around the middle of the MOE (gray, $n = 4$ larvae). (c) The mean number of S100Z-positive cells in the lateral MOE was significantly higher than in the medial MOE ($n = 11$ larvae). Kruskal–Wallis test. **, $p < .01$. (d) The number of S100Z-positive cells in the lateral MOE was always higher than in the medial MOE in all animals investigated ($n = 11$ larvae). (e) The relative position within the MOE on the apical-basal axis was not different between the lateral and medial S100Z-positive populations, a tendency toward a more basal position on the lateral side notwithstanding. (f) The medial S100Z-positive population featured a correlation between the position on the ventral-dorsal and basal-apical axis. Cells deeper in the medial MOE were shifted to apical positions. MOE, main olfactory epithelium.

ORNs that have not yet made axonal contact with the OB of premetamorphic *X. laevis* larvae.

3.5 | Distinct, partially overlapping localization of S100Z and calretinin

We compared the observed S100Z pattern with another Ca^{2+}-binding protein, calretinin (*calb2*). In premetamorphic *X. laevis*, both calretinin and S100Z occurred in ORNs across the whole MOE (Figure 5a). Here, the two Ca^{2+}-binding proteins showed distinct, but partially overlapping, expression patterns (Figure 5a). In the OB, we found axonal projections of calretinin-positive ORNs in glomeruli of the AOB, LC, and MC and calretinin-expressing cell bodies in more posterior OB layers (Figure 5b).

Within the lateral glomerular cluster, individual glomeruli were either positive for calretinin/S100Z or showed a co-localization of both proteins (Figure 5b). The glomerular organization of the LC was different in each animal investigated (Figure 5c). This was also found for the patterns of calretinin and S100Z occurrence in glomeruli. In all larval animals surveyed, we found roughly similar, but never identical, spatial glomerular distribution patterns of calretinin and S100Z (Figure 5c). The most lateral glomeruli of the LC were mostly only S100Z- or calretinin-positive and rarely positive for both (Figure 5c, asterisk). Glomeruli situated toward the center of the LC were more frequently double positive,

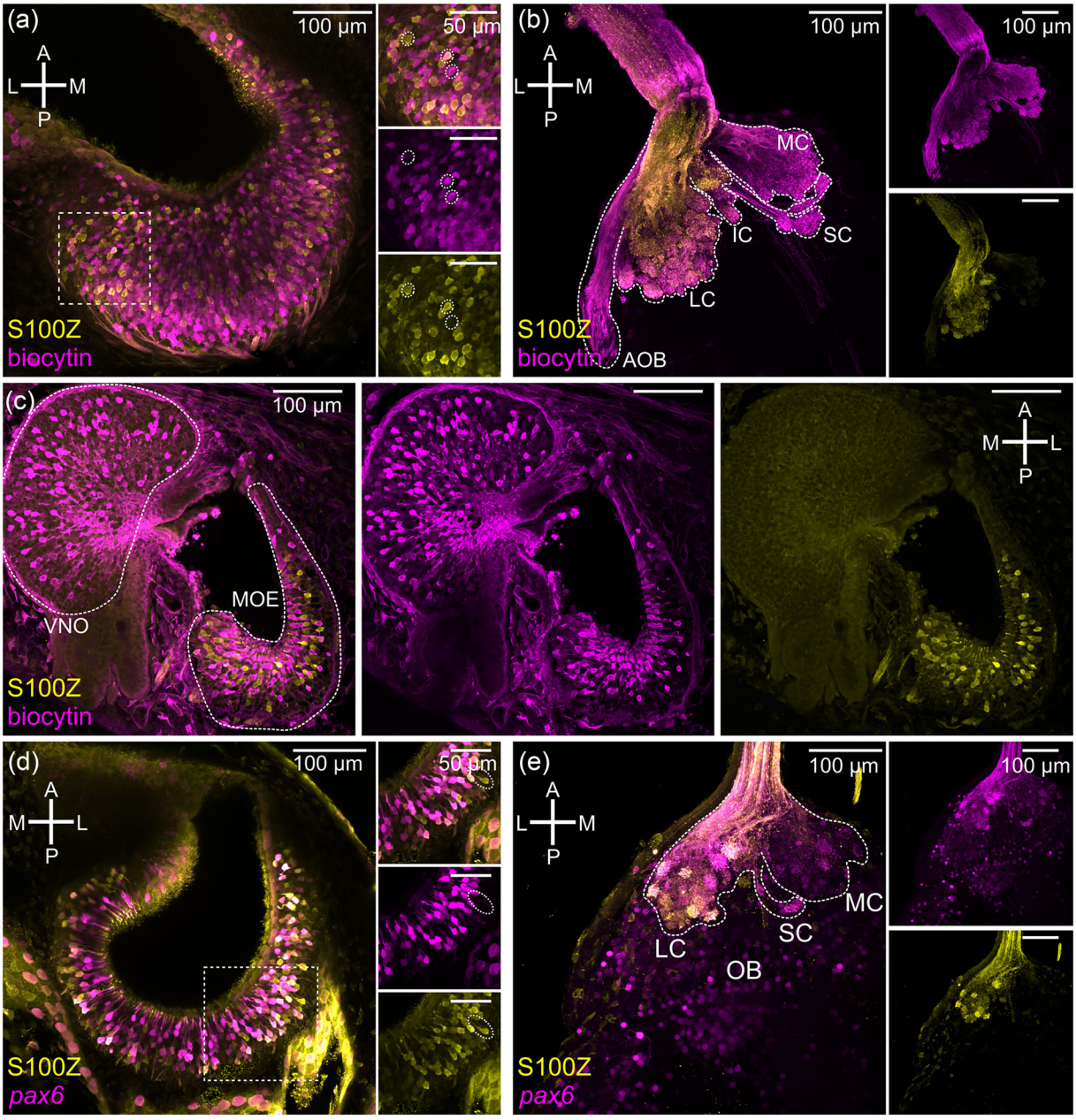

FIGURE 4 Mature and immature receptor neurons express S100Z exclusively in the MOE and not in the VNO of *X. laevis* tadpoles. (a) Biocytin-streptavidin-stained ORNs (magenta) and S100Z-positive ORNs (yellow) were present throughout the whole MOE. Some ORNs showed co-localization with both proteins (highlighted with circles). (b) The axonal projection of biocytin-streptavidin labeled ORNs (magenta) was found in all glomerular clusters within the main OB and AOB of *X. laevis* tadpoles, but axonal projection of S100Z-positive neurons (yellow) was exclusively detected in the LC and IC. (c) Biocytin-streptavidin stained ORNs (magenta) were located in the VNO and MOE of *X. laevis* tadpoles. S100Z-expressing neurons (yellow) occurred in the MOE. (d) Immature *pax6*-positive cells (magenta) and S100Z-positive ORNs (yellow) were present throughout the whole MOE. Although many, not all cells were double positive (e.g., white dotted oval). (e) Axonal projections of *pax6*-positive neurons, indicating an immature status, were detected in the LC and MC within the glomerular layer and different cell types (magenta) within the OB. Some, but not all glomeruli within the LC, showed co-localization for S100Z and *pax6*. A, anterior; AOB, accessory olfactory bulb; IC, intermediate cluster; L, lateral; LC, lateral cluster; M, medial; MC, medial cluster; MOE, main olfactory epithelium; OB, olfactory bulb; ON, olfactory nerve; ORN, olfactory receptor neuron; P, posterior; SC, small cluster; VNO, vomeronasal organ.

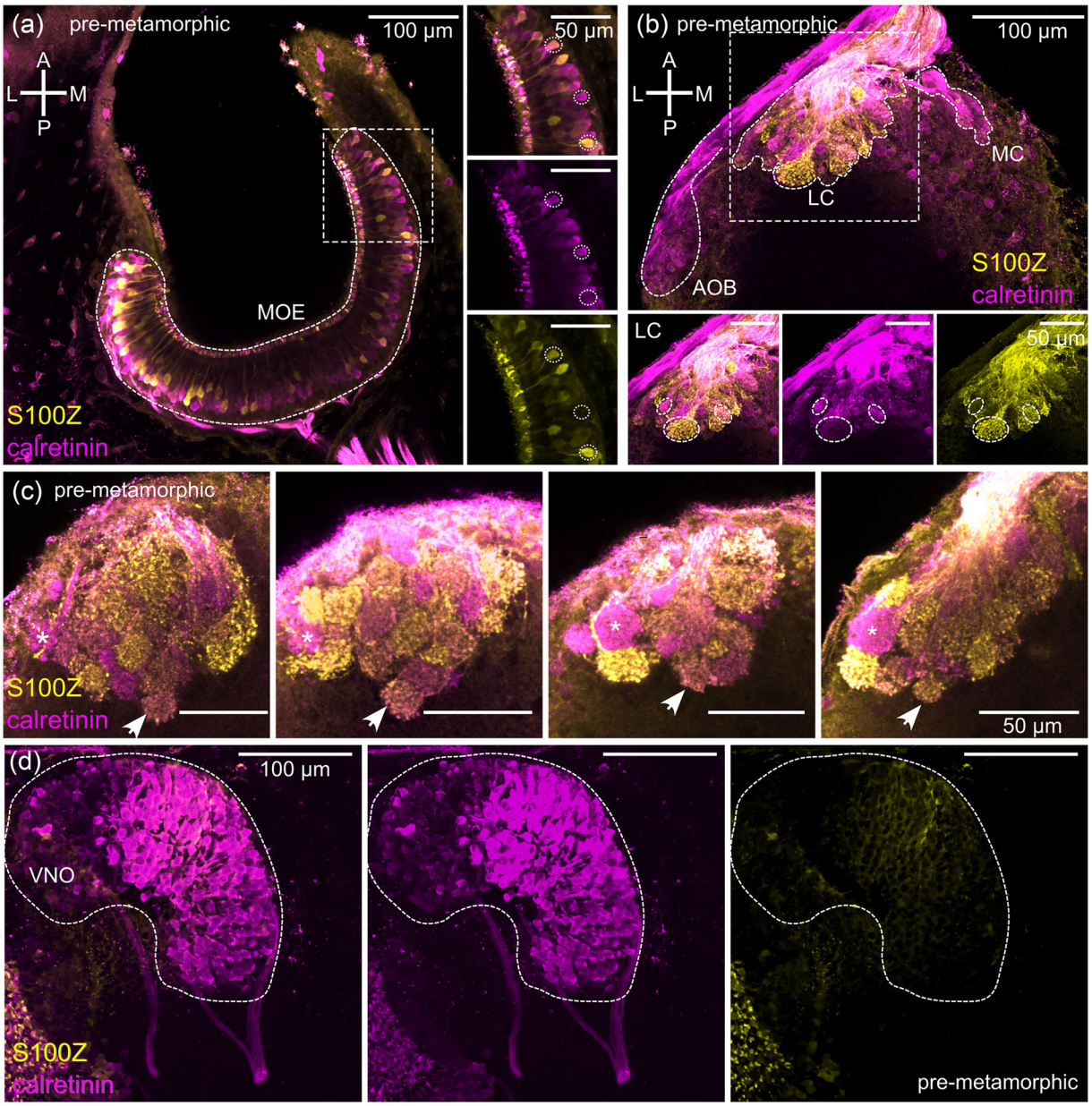

FIGURE 5 Distinct, but partially overlapping expression patterns of calretinin/S100Z. (a) In premetamorphic *X. laevis*, ORNs across the whole MOE expressed calretinin (magenta) and S100Z (yellow). Not all but many cells showed co-localization of the two calcium-binding proteins (e.g., white dotted circles). (b) In premetamorphic animals, the axonal projection of calretinin-expressing neurons (magenta) targeted the AOB, LC, and MC. Within the LC, calretinin- and S100Z-positive (yellow) glomeruli were detected and some were double-positive (white dotted ovals). (c) Expression patterns of calretinin (magenta) and S100Z (yellow) in glomeruli of the lateral cluster in four different premetamorphic animals. The expression patterns were very variable between individuals, but some trends for recurring patterns were apparent. The outer lateral glomeruli within the LC had the tendency to be either S100Z- or calretinin-positive (asterisks), whereas in the medial part of the LC, more glomeruli were S100Z-positive. The most caudal glomerulus in the middle of the LC was often double positive for S100Z/calretinin (arrows). (d) Immunohistochemical staining for calretinin (magenta) labeled neurons throughout the whole VNO in premetamorphic animals, but no S100Z expression (yellow) was found in the VNO. A anterior; AOB, accessory olfactory bulb; L, lateral; LC, lateral cluster; M, medial; MC, medial cluster; MOE, main olfactory epithelium; ORN, olfactory receptor neuron; P, posterior; VNO, vomeronasal organ.

notably a caudally oriented glomerulus was found in many animals (see Figure 5c, arrow). Calretinin expression was also apparent in axons that project to the AOB (Figure 5b). These axons originated from vomeronasal receptor neurons from the VNO that also showed calretinin expression but no S100Z expression (Figure 5d).

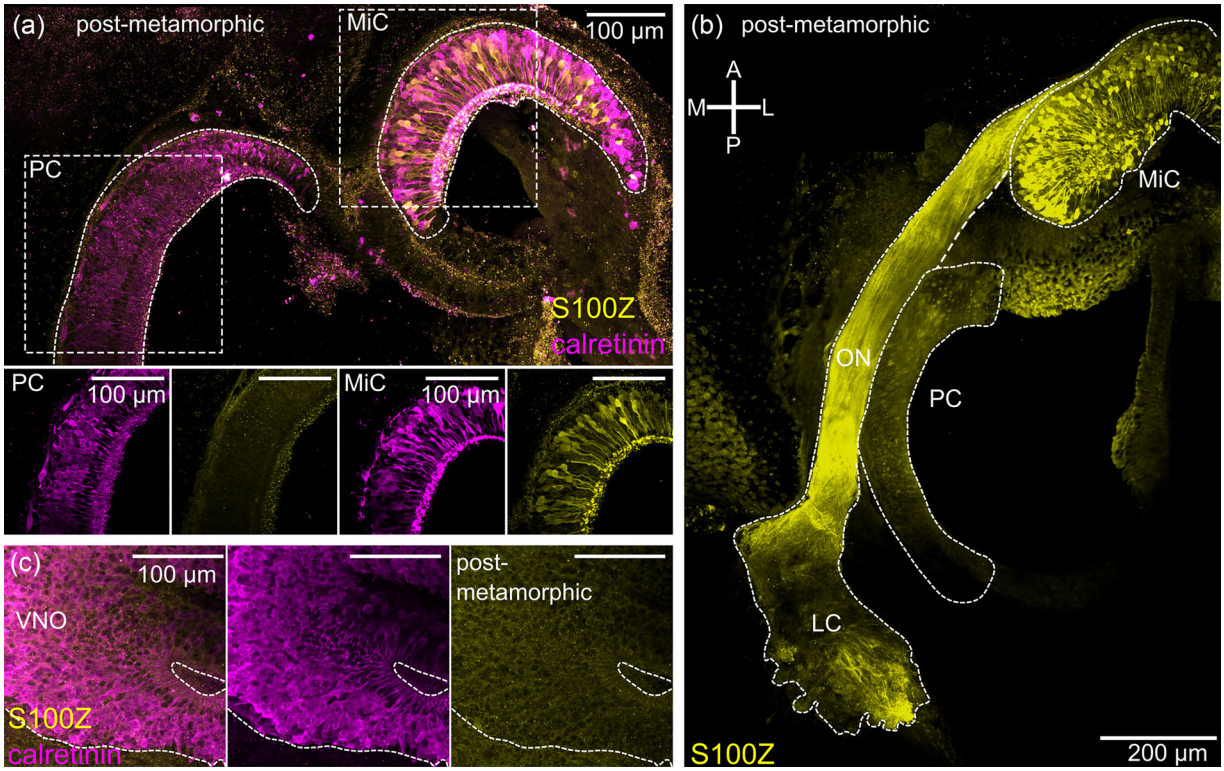

FIGURE 6 S100Z expression restricted to the middle cavity after metamorphosis. (a) In postmetamorphic *X. laevis* calretinin-positive neurons (magenta) were localized in the middle cavity (MiC) and principal cavity (PC). S100Z expression (yellow) occurred only in ORNs of the MiC. (b) In postmetamorphic animals, S100Z-expressing neurons within the olfactory epithelium of the MiC exclusively projected into the lateral glomerular cluster. No expression of S100Z was found in the PC. (c) Immunohistochemical staining for calretinin (magenta) labeled neurons throughout the whole VNO in postmetamorphic animals. No S100Z expression (yellow) was detected in the VNO. A, anterior; L, lateral; LC, lateral cluster; M, medial; MiC, middle cavity; ON, olfactory nerve; ORN, olfactory receptor neuron; P, posterior; PC, principal cavity; VNO, vomeronasal organ.

3.6 | S100Z expression limited to the middle cavity after metamorphosis

During metamorphic remodeling of the olfactory system, the larval MOE is functionally reorganized in the principal cavity , and a new olfactory epithelium forms the middle cavity (for review, see Weiss et al., 2021). The air-filled principal cavity is thought to be specialized for airborne odor detection, whereas the middle cavity is a reproduced larval MOE presumably specialized for waterborne odor detection. After metamorphosis, we found calretinin in ORNs of the middle and principal cavity of the olfactory system, whereas S100Z-expressing neurons were only detectable in the middle cavity (Figure 6a). Comparable to the larval situation, S100Z-expressing ORNs from the middle cavity exclusively projected into the lateral glomerular cluster of the postmetamorphic OB (Figure 6b). Also, no expression of S100Z occurred in the VNO (Figure 6c). Calretinin, on the other hand, could be detected in neurons of the VNO (Figure 6c).

4 | DISCUSSION

4.1 | S100Z expression in the olfactory system

The Ca^{2+}-binding protein family S100 has only been found in vertebrates and is expressed non-ubiquitously (Gonzalez et al., 2020). Although not very well characterized, S100Z has been shown to be expressed in the olfactory system of fish and mammals (Capsoni et al., 2021; Dieris et al., 2021; Hecker et al., 2019; Kraemer et al., 2008). Antibodies against bovine S100A/S100B reveal S100-immunoreactivity in crypt cells of the fish olfactory rosette and are a recognized marker for this neuronal subtype (Bettini et al., 2017; Germanà et al., 2004). Crypt cells express a single *v1r*-related *ora* gene (Oka et al., 2012), and they converge into a single mediodorsal glomerulus that is activated by kin odor after olfactory imprinting (Ahuja et al., 2013; Biechl et al., 2017; Gayoso et al., 2012; Kress et al., 2015). The specificity of these antibodies has been reported to be highly sensitive to sample preparation

prior to immunolabeling, and with this ambiguity also, other microvillous-like olfactory neurons are labeled (Oka et al., 2012). Therefore, the interpretation of earlier reports on S100 expression in non-mammalian species is not straightforward. In fact, it has been shown that zebrafish crypt cells do not even express *s100* genes and that the antibody may recognize a non-S100 protein, whereas in microvillous-like cells, the antibody actually labels S100Z (Ahuja et al., 2013; Oka et al., 2012). The same antibody has been also shown to label ORNs in larval *X. laevis* (Kerschbaum & Hermann, 1992). Using another antibody raised specifically against *H. sapiens* S100Z, we found labeling in a restricted population of ORNs of the main olfactory system of *X. laevis*. We have performed large-scale RNAseq experiments that support our findings (Data unpublished). A binding protein of S100 occurs in olfactory neuron cilia of another anuran, *Rana catesbeiana*, and thus suggests a role in olfactory transduction (Miwa & Kawamura, 2003).

4.2 | Partially overlapping expression of Ca^{2+}-binding proteins

Generally, many members of different Ca^{2+}-binding protein subfamilies are expressed in a restricted pattern and serve as a marker for separate neuronal populations in the vertebrate central nervous system (Braubach et al., 2012; Kress et al., 2015; Morona & González, 2013). In the olfactory system, calretinin expression is restricted to neuronal cell populations (Germanà et al., 2007). In zebrafish, calretinin is found most strongly in ciliated olfactory sensory neurons, which broadly project to the OB (Braubach et al., 2012; Kress et al., 2015; but see Koide et al., 2009). In this study, most ORNs of the *Xenopus* MOE were calretinin-positive (see also Daume et al., 2022).

In fish and amphibians, calretinin is an accepted marker of mature ORNs, but calretinin expression in embryonic mice is restricted to a limited period during neuronal maturation (Wei et al., 2013). A neuroprotective function of calretinin is proposed for epileptic seizures, but the function of calretinin in the olfactory system remains unclear (Capsoni et al., 2021; Qi et al., 2022).

We cannot link calretinin expression to specific neuronal features or identities, and no clear pattern of co-expression with S100Z was found. Furthermore, we did not observe any consistent expression patterns across the glomerular array in different animals. This implies that the mapping of ORN populations expressing these proteins in the *Xenopus* OB is not stereotypical. This inference is backed by functional measurements, which demonstrate that the glomerular odor map to amino acid odorants is neither stereotypically or chemotopically arranged in the *Xenopus* OB (Offner et al., 2023). We observed one particular, caudally oriented glomerulus in the LC, which was S100Z/calretinin-positive in many animals. It will be interesting to investigate if this glomerulus features some stereotypical properties, like location, function or odor sensitivity.

4.3 | S100Z is not associated with the VNO in *Xenopus*

In mammals, *s100z* has previously been associated with the accessory olfactory system, particularly the VNO. Surprisingly, we did not detect any S100Z expression in the VNO of pre- nor postmetamorphic *Xenopus*. In a large-scale screening of mammalian genomes, it was found that a reduction of the vomeronasal system is accompanied by a convergent inactivation of *s100z*, the transduction channel *trpc2*, the aldehyde oxidase *Aox2* involved in odorant degradation, and the uncharacterized *Mslnl* (Hecker et al., 2019). Conversely, the inactivation of these genes predicts a vomeronasal system reduction in semi-aquatic mammals, namely, otters and phocid seals (Hecker et al., 2019).

Ecological factors such as the terrestrial or aquatic environment can influence the evolution of olfactory system adaptations (Burguera et al., 2023; Kishida, 2021; Weiss et al., 2021). The functional prioritization of selected components of the olfactory system is common among vertebrates and can lead to the enhanced or decreased expression of particular families of olfactory receptor genes (Bear et al., 2016; Kishida, 2021; Taniguchi & Taniguchi, 2014). For instance, multiple lineages of ray-finned fish have independently expanded their olfactory receptor gene families, and this expansion is especially evident in nocturnal amphibious fish (Burguera et al., 2023). Such changes can also result in alterations to the occurrence of cellular properties that are associated with either the main or accessory olfactory system. In cartilaginous fish, the v2r/OlfC family of olfactory receptor genes is dominant over the OR family, and only microvillous ORNs are present in the olfactory organ (Syed et al., 2023).

The most extreme adaptation of the olfactory system completely reduces either the main or accessory system in favor of the other. Among secondarily fully aquatic mammals, baleen whales (Mysticeti) possess only a reduced main olfactory organ and lack a VNO (Kishida et al., 2015). No VNO is apparent in birds, so they depend entirely on their sense of smell through the main olfactory system (Taniguchi & Taniguchi, 2014). On the other hand, fully aquatic sea snakes (Hydrophiins) lack a functional main olfactory system and instead rely on a vomeronasal system (Kishida, 2021).

Our study emphasizes that the expression of *s100z* in non-mammalian species cannot be directly linked to the VNO. This makes *s100z* a less reliable predictor for a reduction of the VNO as a whole or the molecular machinery connected to it. It will be interesting to investigate the *s100z*

expression in animals with olfactory system reductions and other non-mammalian vertebrates in general.

4.4 | S100Z expression pattern correlates with microvillous ORNs and *trpc2*

In non-tetrapod groups, without a distinct VNO, the expression of *trpc2* is still linked to the MOE (Bear et al., 2016). In the MOE, the major two neuronal subpopulations are ciliated and microvillous ORNs (Gliem et al., 2013). In the single olfactory sensory epithelium of bony and cartilaginous fishes, *trpc2* is expressed in microvillous ORNs (Sato et al., 2005; Syed et al., 2023). In early diverging tetrapods, like amphibians, the expression pattern is in an intermediate state. In larval *Xenopus*, *trpc2* expression is not restricted to the VNO but also occurs broadly in the MOE (Sansone, Syed, et al., 2014). After metamorphosis, *trpc2* is expressed in the VNO and in the olfactory epithelium of the water-exposed middle cavity but not in the air-exposed principal cavity (Syed et al., 2017). The pattern in the MOE is mirrored by our observed expression pattern of S100Z. This indicates a common cellular identity that expresses S100Z and TRPC2, at least partially overlapping.

We found indications that S100Z-positive ORNs possess no cilia and that further supports that they belong to the microvillous subpopulation. Also, the absence of S100Z-positive cells in the postmetamorphic principal cavity supports this fact. After metamorphic reorganization, no microvillous, but only ciliated ORNs, can be found in the principal cavity (Hansen et al., 1998). It is unclear if S100Z is expressed by the whole population of microvillous ORNs in the MOE.

Microvillous ORNs expressing *trpc2* are thought to share a common molecular identity with a non-cyclic adenosine monophosphate (cAMP)-dependent transduction pathway and expression of early-derived *v2r* family olfactory receptor genes (Gliem et al., 2013; Hansen et al., 2004; Sato et al., 2005; Syed et al., 2013, 2017). Interestingly, microvillous ORNs from the MOE and the VNO of *X. laevis* express distinct subfamilies of *v2r* genes. *Xenopus* larvae show exclusive expression of late diverging *v2r* genes in the VNO, while ancestral *v2r* genes are restricted to the MOE (Syed et al., 2013). During metamorphosis, the MOE gradually loses its larval expression of ancient V2Rs as it transforms into the air nose (principal cavity). In the basal layers of the newly formed water nose (middle cavity), ancient *v2r* gene expression starts to emerge (Syed et al., 2017). This suggests ancestral *v2r* olfactory receptor genes as likely candidates to be expressed by S100Z-positive ORNs. This is an important hypothesis to test in future experiments.

The functional identity of S100Z-expressing ORNs is not known yet, but V2Rs have been connected to the detection of amino acids (DeMaria et al., 2013; Syed et al., 2017). In larval *Xenopus*, amino acid-responsive ORNs with a phospholipase C (PLC)-dependent transduction pathway show a laterally biased distribution (Gliem et al., 2013; Sansone, Hassenklöver, et al., 2014; Sansone, Syed, et al., 2014; Syed et al., 2013). This lateral bias is also present in the glomerular array of the OB (Gliem et al., 2013). Since S100Z expression in the OB is also lateralized, it would be interesting to test whether S100Z-positive glomeruli are sensitive to amino acid odors.

4.5 | Conclusion

The transition to terrestrial habitats of tetrapods is accompanied by the evolutionary tendency to develop distinct olfactory subsystems, for example, the main and vomeronasal olfactory organ with separate brain circuitry. This trend at the anatomical level is also reflected at the molecular level, which eventually forms distinct olfactory sensory neuron subpopulations with differential gene expression patterns. In amphibians, this molecular segregation is in an intermediate state, despite distinct anatomical peripheral olfactory organs. This is also supported by strict S100Z expression in the main olfactory system and no expression in the VNO. This underlines that the molecular identity of amphibian vomeronasal olfactory neurons is not identical to mammals, including the expression of S100Z. Since the function of *s100z* is still unclear, one can only speculate about the consequences. A functional importance in a specific olfactory neuron subpopulation could be hypothesized and it is possible that the association of *s100z* with vomeronasal sensory neurons in the mammalian lineage confers functional benefits.

AUTHOR CONTRIBUTIONS

Melina Kahl: Conceptualization; formal analysis; investigation; writing—original draft; writing—review and editing; visualization. **Thomas Offner**: Conceptualization; formal analysis; writing—review and editing. **Alena Trendel**: Formal analysis. **Lukas Weiss**: Investigation; writing—review and editing. **Ivan Manzini**: Conceptualization; writing—review and editing; supervision; funding acquisition. **Thomas Hassenklöver**: Conceptualization; formal analysis; writing—original draft; writing—review and editing; visualization; supervision.

ACKNOWLEDGMENTS

The authors thank Christina Anding for expert animal care and Anja Schnecko for technical assistance. This work was supported by Deutsche Forschungsgemeinschaft (DFG) grant 4113/4-1.

Open access funding enabled and organized by Projekt DEAL.

CONFLICT OF INTEREST STATEMENT

The authors declare no competing interests.

DATA AVAILABILITY STATEMENT

The data that support the findings of this study are openly available in JLUpub at https://doi.org/10.22029/jlupub-18280.

ORCID

Melina Kahl https://orcid.org/0009-0006-6223-770X
Thomas Offner https://orcid.org/0000-0002-0228-2545
Lukas Weiss https://orcid.org/0000-0003-3078-8006
Ivan Manzini https://orcid.org/0000-0002-3575-9637
Thomas Hassenklöver https://orcid.org/0000-0002-9895-1263

REFERENCES

Ahuja, G., Ivandić, I., Saltürk, M., Oka, Y., Nadler, W., & Korsching, S. I. (2013). Zebrafish crypt neurons project to a single, identified mediodorsal glomerulus. *Scientific Reports*, *3*, 2063. https://doi.org/10.1038/srep02063

Bear, D. M., Lassance, J.-M., Hoekstra, H. E., & Datta, S. R. (2016). The evolving neural and genetic architecture of vertebrate olfaction. *Current Biology*, *26*, R1039–R1049. https://doi.org/10.1016/j.cub.2016.09.011

Berridge, M. J., Bootman, M. D., & Roderick, H. L. (2003). Calcium signalling: Dynamics, homeostasis and remodelling. *Nature Reviews Molecular Cell Biology*, *4*, 517–529. https://doi.org/10.1038/nrm1155

Berridge, M. J., Lipp, P., & Bootman, M. D. (2000). The versatility and universality of calcium signalling. *Nature Reviews Molecular Cell Biology*, *1*, 11–21. https://doi.org/10.1038/35036035

Bettini, S., Milani, L., Lazzari, M., Maurizii, M. G., & Franceschini, V. (2017). Crypt cell markers in the olfactory organ of *Poecilia reticulata*: Analysis and comparison with the fish model *Danio rerio*. *Brain Structure and Function*, *222*, 3063–3074. https://doi.org/10.1007/s00429-017-1386-2

Biechl, D., Tietje, K., Ryu, S., Grothe, B., Gerlach, G., & Wullimann, M. F. (2017). Identification of accessory olfactory system and medial amygdala in the zebrafish. *Scientific Reports*, *7*, 44295. https://doi.org/10.1038/srep44295

Braubach, O. R., Fine, A., & Croll, R. P. (2012). Distribution and functional organization of glomeruli in the olfactory bulbs of zebrafish (*Danio rerio*). *Journal of Comparative Neurology*, *520*, 2317–2339. https://doi.org/10.1002/cne.23075

Burguera, D., Dionigi, F., Kverková, K., Winkler, S., Brown, T., Pippel, M., Zhang, Y., Shafer, M., Nichols, A. L. A., Myers, E., Němec, P., & Musilova, Z. (2023). Expanded olfactory system in ray-finned fishes capable of terrestrial exploration. *BMC Biology*, *21*, 163. https://doi.org/10.1186/s12915-023-01661-8

Capsoni, S., Iseppe, A. F., Casciano, F., & Pignatelli, A. (2021). Unraveling the role of dopaminergic and calretinin interneurons in the olfactory bulb. *Frontiers in Neural Circuits*, *15*, 718221. https://doi.org/10.3389/fncir.2021.718221

Carafoli, E., Santella, L., Branca, D., & Brini, M. (2001). Generation, control, and processing of cellular calcium signals. *Critical Reviews in Biochemistry and Molecular Biology*, *36*, 107–260. https://doi.org/10.1080/20014091074183

Cervino, A. S., Paz, D. A., & Frontera, J. L. (2017). Neuronal degeneration and regeneration induced by axotomy in the olfactory epithelium of *Xenopus laevis*. *Developmental Neurobiology*, *77*, 1308–1320. https://doi.org/10.1002/dneu.22513

Date-Ito, A., Ohara, H., Ichikawa, M., Mori, Y., & Hagino-Yamagishi, K. (2008). *Xenopus* V1R vomeronasal receptor family is expressed in the main olfactory system. *Chemical Senses*, *33*, 339–346. https://doi.org/10.1093/chemse/bjm090

Daume, D., Offner, T., Hassenklöver, T., & Manzini, I. (2022). Patterns of *tubb2b* promoter-driven fluorescence in the forebrain of larval *Xenopus laevis*. *Frontiers in Neuroanatomy*, *16*, 914281. https://doi.org/10.3389/fnana.2022.914281

DeMaria, S., Berke, A. P., Name, E. V., Heravian, A., Ferreira, T., & Ngai, J. (2013). Role of a ubiquitously expressed receptor in the vertebrate olfactory system. *Journal of Neuroscience*, *33*, 15235–15247. https://doi.org/10.1523/jneurosci.2339-13.2013

Dieris, M., Kowatschew, D., & Korsching, S. I. (2021). Olfactory function in the trace amine-associated receptor family (TAARs) evolved twice independently. *Scientific Reports*, *11*, 7807. https://doi.org/10.1038/s41598-021-87236-5

Donato, R. (2003). Intracellular and extracellular roles of S100 proteins. *Microscopy Research and Technique*, *60*, 540–551. https://doi.org/10.1002/jemt.10296

Elíes, J., Yáñez, M., Pereira, T. M. C., Gil-Longo, J., MacDougall, D. A., & Campos-Toimil, M. (2019). An update to calcium binding proteins. In M. Islam (Ed.), *Advances in experimental medicine and biology*. (pp. 183–213). Springer International Publishing. https://doi.org/10.1007/978-3-030-12457-1_8

Gayoso, J., Castro, A., Anadón, R., & Manso, M. J. (2012). Crypt cells of the zebrafish *Danio rerio* mainly project to the dorsomedial glomerular field of the olfactory bulb. *Chemical Senses*, *37*, 357–369. https://doi.org/10.1093/chemse/bjr109

Germanà, A., Montalbano, G., Laurà, R., Ciriaco, E., del Valle, M. E., & Vega, J. A. (2004). S100 protein-like immunoreactivity in the crypt olfactory neurons of the adult zebrafish. *Neuroscience Letters*, *371*, 196–198. https://doi.org/10.1016/j.neulet.2004.08.077

Germanà, A., Paruta, S., Germanà, G. P., Ochoa-Erena, F. J., Montalbano, G., Cobo, J., & Vega, J. A. (2007). Differential distribution of S100 protein and calretinin in mechanosensory and chemosensory cells of adult zebrafish (*Danio rerio*). *Brain Research*, *1162*, 48–55. https://doi.org/10.1016/j.brainres.2007.05.070

Gliem, S., Syed, A. S., Sansone, A., Kludt, E., Tantalaki, E., Hassenklöver, T., Korsching, S. I., & Manzini, I. (2013). Bimodal processing of olfactory information in an amphibian nose: Odor responses segregate into a medial and a lateral stream. *Cellular and Molecular Life Sciences*, *70*, 1965–1984. https://doi.org/10.1007/s00018-012-1226-8

Gonzalez, L. L., Garrie, K., & Turner, M. D. (2020). Role of S100 proteins in health and disease. *Biochimica et Biophysica Acta (BBA)—Molecular Cell Research*, *1867*, 118677. https://doi.org/10.1016/j.bbamcr.2020.118677

Hansen, A., Anderson, K. T., & Finger, T. E. (2004). Differential distribution of olfactory receptor neurons in goldfish: Structural and molecular correlates. *Journal of Comparative Neurology*, *477*, 347–359. https://doi.org/10.1002/cne.20202

Hansen, A., Reiss, J. O., Gentry, C. L., & Burd, G. D. (1998). Ultrastructure of the olfactory organ in the clawed frog, *Xenopus laevis*,

during larval development and metamorphosis. *Journal of Comparative Neurology*, *398*, 273–288. https://doi.org/10.1002/(SICI)1096-9861(19980824)398:2⟨273::AID-CNE8⟩3.0.CO;2-Y

Hecker, N., Lächele, U., Stuckas, H., Giere, P., & Hiller, M. (2019). Convergent vomeronasal system reduction in mammals coincides with convergent losses of calcium signalling and odorant-degrading genes. *Molecular Ecology*, *28*, 3656–3668. https://doi.org/10.1111/mec.15180

Hermann, A., Donato, R., Weiger, T. M., & Chazin, W. J. (2012). S100 calcium binding proteins and ion channels. *Frontiers in Pharmacology*, *3*, 67. https://doi.org/10.3389/fphar.2012.00067

Kerschbaum, H. H., & Hermann, A. (1992). Calcium-binding proteins in chemoreceptors of *Xenopus laevis*. *Tissue & Cell*, *24*, 719–724. https://doi.org/10.1016/0040-8166(92)90043-7

Kishida, T. (2021). Olfaction of aquatic amniotes. *Cell and Tissue Research*, *383*, 353–365. https://doi.org/10.1007/s00441-020-03382-8

Kishida, T., Thewissen, J., Hayakawa, T., Imai, H., & Agata, K. (2015). Aquatic adaptation and the evolution of smell and taste in whales. *Zoological Letters*, *1*, 9. https://doi.org/10.1186/s40851-014-0002-z

Koide, T., Miyasaka, N., Morimoto, K., Asakawa, K., Urasaki, A., Kawakami, K., & Yoshihara, Y. (2009). Olfactory neural circuitry for attraction to amino acids revealed by transposon-mediated gene trap approach in zebrafish. *Proceedings of the National Academy of Sciences*, *106*, 9884–9889. https://doi.org/10.1073/pnas.0900470106

Kraemer, A. M., Saraiva, L. R., & Korsching, S. I. (2008). Structural and functional diversification in the teleost S100 family of calcium-binding proteins. *BMC Evolutionary Biology*, *8*, 48. https://doi.org/10.1186/1471-2148-8-48

Kress, S., Biechl, D., & Wullimann, M. F. (2015). Combinatorial analysis of calcium-binding proteins in larval and adult zebrafish primary olfactory system identifies differential olfactory bulb glomerular projection fields. *Brain Structure and Function*, *220*, 1951–1970. https://doi.org/10.1007/s00429-014-0765-1

Miwa, N., & Kawamura, S. (2003). Frog p26olf, a molecule with two S100-like regions in a single peptide. *Microscopy Research and Technique*, *60*, 593–599. https://doi.org/10.1002/jemt.10301

Mohrhardt, J., Nagel, M., Fleck, D., Ben-Shaul, Y., & Spehr, M. (2018). Signal detection and coding in the accessory olfactory system. *Chemical Senses*, *43*, 667–695. https://doi.org/10.1093/chemse/bjy061

Moreno, N., Rétaux, S., & González, A. (2008). Spatio-temporal expression of Pax6 in *Xenopus* forebrain. *Brain Research*, *1239*, 92–99. https://doi.org/10.1016/j.brainres.2008.08.052

Morona, R., & González, A. (2013). Pattern of calbindin-D28k and calretinin immunoreactivity in the brain of *Xenopus laevis* during embryonic and larval development. *Journal of Comparative Neurology*, *521*, 79–108. https://doi.org/10.1002/cne.23163

Nieuwkoop, P. D., & Faber, J. (Eds.). (1994). *Normal table of Xenopus laevis (Daudin)*. Garland Science.

Offner, T., Weiss, L., Daume, D., Berk, A., Inderthal, T. J., Manzini, I., & Hassenklöver, T. (2023). Functional odor map heterogeneity is based on multifaceted glomerular connectivity in larval Xenopus olfactory bulb. *iScience*, *26*, 107518. https://doi.org/10.1016/j.isci.2023.107518

Oka, Y., Saraiva, L. R., & Korsching, S. I. (2012). Crypt neurons express a single *v1r*-related *ora* gene. *Chemical Senses*, *37*, 219–227. https://doi.org/10.1093/chemse/bjr095

Preibisch, S., Saalfeld, S., & Tomancak, P. (2009). Globally optimal stitching of tiled 3D microscopic image acquisitions. *Bioinformatics*, *25*, 1463–1465. https://doi.org/10.1093/bioinformatics/btp184

Qi, Y., Cheng, H., Wang, Y., & Chen, Z. (2022). Revealing the precise role of calretinin neurons in epilepsy: We are on the way. *Neuroscience Bulletin*, *38*, 209–222. https://doi.org/10.1007/s12264-021-00753-1

Sansone, A., Hassenklöver, T., Syed, A. S., Korsching, S. I., & Manzini, I. (2014). Phospholipase C and diacylglycerol mediate olfactory responses to amino acids in the main olfactory epithelium of an amphibian. *PLoS ONE*, *9*, e87721. https://doi.org/10.1371/journal.pone.0087721

Sansone, A., Syed, A. S., Tantalaki, E., Korsching, S. I., & Manzini, I. (2014). *Trpc2* is expressed in two olfactory subsystems, the main and the vomeronasal system of larval *Xenopus laevis*. *Journal of Experimental Biology*, *217*, 2235–2238. https://doi.org/10.1242/jeb.103465

Santamaria-Kisiel, L., Rintala-Dempsey, A. C., & Shaw, G. S. (2006). Calcium-dependent and -independent interactions of the S100 protein family. *Biochemical Journal*, *396*, 201–214. https://doi.org/10.1042/bj20060195

Sato, Y., Miyasaka, N., & Yoshihara, Y. (2005). Mutually exclusive glomerular innervation by two distinct types of olfactory sensory neurons revealed in transgenic zebrafish. *Journal of Neuroscience*, *25*, 4889–4897. https://doi.org/10.1523/jneurosci.0679-05.2005

Schindelin, J., Arganda-Carreras, I., Frise, E., Kaynig, V., Longair, M., Pietzsch, T., Preibisch, S., Rueden, C., Saalfeld, S., Schmid, B., Tinevez, J. Y., White, D. J., Hartenstein, V., Eliceiri, K., Tomancak, P., & Cardona, A. (2012). Fiji: An open-source platform for biological-image analysis. *Nature Methods*, *9*, 676–682. https://doi.org/10.1038/nmeth.2019

Schnittke, N., Herrick, D. B., Lin, B., Peterson, J., Coleman, J. H., Packard, A. I., Jang, W., & Schwob, J. E. (2015). Transcription factor p63 controls the reserve status but not the stemness of horizontal basal cells in the olfactory epithelium. *Proceedings of the National Academy of Sciences of the United States of America*, *112*(36), E5068–E5077. https://doi.org/10.1073/pnas.1512272112

Schwaller, B. (2020). Cytosolic Ca^{2+} buffers are inherently Ca^{2+} signal modulators. *Cold Spring Harbor perspectives in biology*, *12*, a035543. https://doi.org/10.1101/cshperspect.a035543

Singh, P., & Ali, S. A (2022). Multifunctional role of S100 protein family in the immune system: An update. *Cells*, *11*, 2274. https://doi.org/10.3390/cells11152274

Stoykova, A., & Gruss, P. (1994). Roles of Pax-genes in developing and adult brain as suggested by expression patterns. *Journal of Neuroscience*, *14*, 1395–1412. https://doi.org/10.1523/jneurosci.14-03-01395.1994

Syed, A. S., Sansone, A., Hassenklöver, T., Manzini, I., & Korsching, S. I. (2017). Coordinated shift of olfactory amino acid responses and V2R expression to an amphibian water nose during metamorphosis. *Cellular and Molecular Life Sciences*, *74*, 1711–1719. https://doi.org/10.1007/s00018-016-2437-1

Syed, A. S., Sansone, A., Nadler, W., Manzini, I., & Korsching, S. I. (2013). Ancestral amphibian v2rs are expressed in the main olfactory epithelium. *Proceedings of the National Academy of Sciences*, *110*, 7714–7719. https://doi.org/10.1073/pnas.1302088110

Syed, A. S., Sharma, K., Policarpo, M., Ferrando, S., Casane, D., & Korsching, S. I. (2023). Ancient and nonuniform loss of olfactory

receptor expression renders the shark nose a de facto vomeronasal organ. *Molecular Biology and Evolution*, *40*, msad076. https://doi.org/10.1093/molbev/msad076

Taniguchi, K., & Taniguchi, K. (2014). Phylogenic studies on the olfactory system in vertebrates. *Journal of Veterinary Medical Science*, *76*, 781–788. https://doi.org/10.1292/jvms.13-0650

Wei, H., Lang, M.-F., & Jiang, X. (2013). Calretinin is expressed in the intermediate cells during olfactory receptor neuron development. *Neuroscience Letters*, *542*, 42–46. https://doi.org/10.1016/j.neulet.2013.03.022

Weiss, L., Manzini, I., & Hassenklöver, T. (2021). Olfaction across the water–air interface in anuran amphibians. *Cell and Tissue Research*, *383*, 301–325. https://doi.org/10.1007/s00441-020-03377-5

Yáñez, M., Gil-Longo, J., & Campos-Toimil, M. (2012). Calcium binding proteins. In *Calcium Signaling* (pp. 461–482). Springer Netherlands. https://doi.org/10.1007/978-94-007-2888-2_19

How to cite this article: Kahl, M., Offner, T., Trendel, A., Weiss, L., Manzini, I., & Hassenklöver, T. (2024). S100Z is expressed in a lateral subpopulation of olfactory receptor neurons in the main olfactory system of *Xenopus laevis*. *Developmental Neurobiology*, *84*, 59–73. https://doi.org/10.1002/dneu.22935